The petrochemistry of the Lower Proterozoic metamorphic rocks from the Dabieshan–Lianyungang area, the southeastern margin of the North China Platform

SANG LONGKANG

China University of Geosciences, Wuhan 430074, P.R. China

Abstract

Based on geological studies, 141 rock analyses and 5 trace element analyses of metabasites, the present paper deals with the rock association, chemical features, protolith formation and the original tectonic settings upwards through the Lower Proterozoic metamorphic strata in the Dabieshan–Lianyungang area, in the south-east of the North China Platform. The results of the study indicate that the lower and middle parts of the metamorphic strata comprise terrigenous clastics, phosphoritic and aluminous sedimentary formations which formed under stable continental margin conditions. In the middle–upper part a calc-alkaline volcano–sedimentary formation under the active continental margin was developed. The Lower Proterozoic meta-strata of sedimentary–volcanosedimentary origin from bottom upwards suggest that the tectonic evolution of the south-eastern margin of the North China Platform is a process from stabilization to mobilization. This process suggests a northward subduction of the Yangtze Plate under the North China Plate during the later part of the early Proterozoic.

KEYWORDS: metabasites, petrochemistry, North China Platform.

Introduction

THE Dabieshan area of Hubei, Henan and Anhui Provinces and the Lianyungang area of Jiangsu province is tectonically situated on the south-eastern margin of the North China Platform. In these areas the Precambrian regional metamorphic rocks are widely distributed. It is about 96000 km^2 in area. The NNE-trending Tanlu fault cuts through it with an offset about 400 km, separating it into two parts. The well-known early Proterozoic Jiangsu–Anhui–Hubei phosphorite ore belt and late Proterozoic Mulanshan–Zhangbaling blueschist belt are located in these areas (Fig. 1). However, most of the previous work (Xu *et al.*, 1986; Suo *et al.*, 1988) was concentrated on tectonic problems; metamorphic petrochemistry has not been systematically studied. Based on the field occurrence and petrochemical studies, the stratigraphic subdivision, the association of metamorphic rocks, petrochemistry and protolith formation of the Lower Proterozoic metamorphic rocks and the tectonic evolution of the early Proterozoic time are discussed in this paper.

The general characteristics of the Lower Proterozoic metastrata

Surface studies and drilling have revealed that the stratigraphy of the Dabieshan and the Lianyungang areas, though separated by the NNE-trending Tanlu fault, are well correlated. Both can be subdivided into three rock suites, namely the Upper Proterozoic blueschist belt, Lower Proterozoic phosphoritic belt and Upper Archaean gneiss–migmatitc complex (Fig. 1). They are significantly different in isotopic dating, rock association, metamorphism and relevant ore deposits (Table 1).

The Lower Proterozoic rocks occur from Dawu Hubei eastwards through Susong Anhei to Lianyungang Jiangsu Province (Fig. 1). They unconformably overlie the Upper Archaean and fault contact with the Upper Proterozoic. Five

Mineralogical Magazine, June 1991, Vol. 55, pp. 263–276

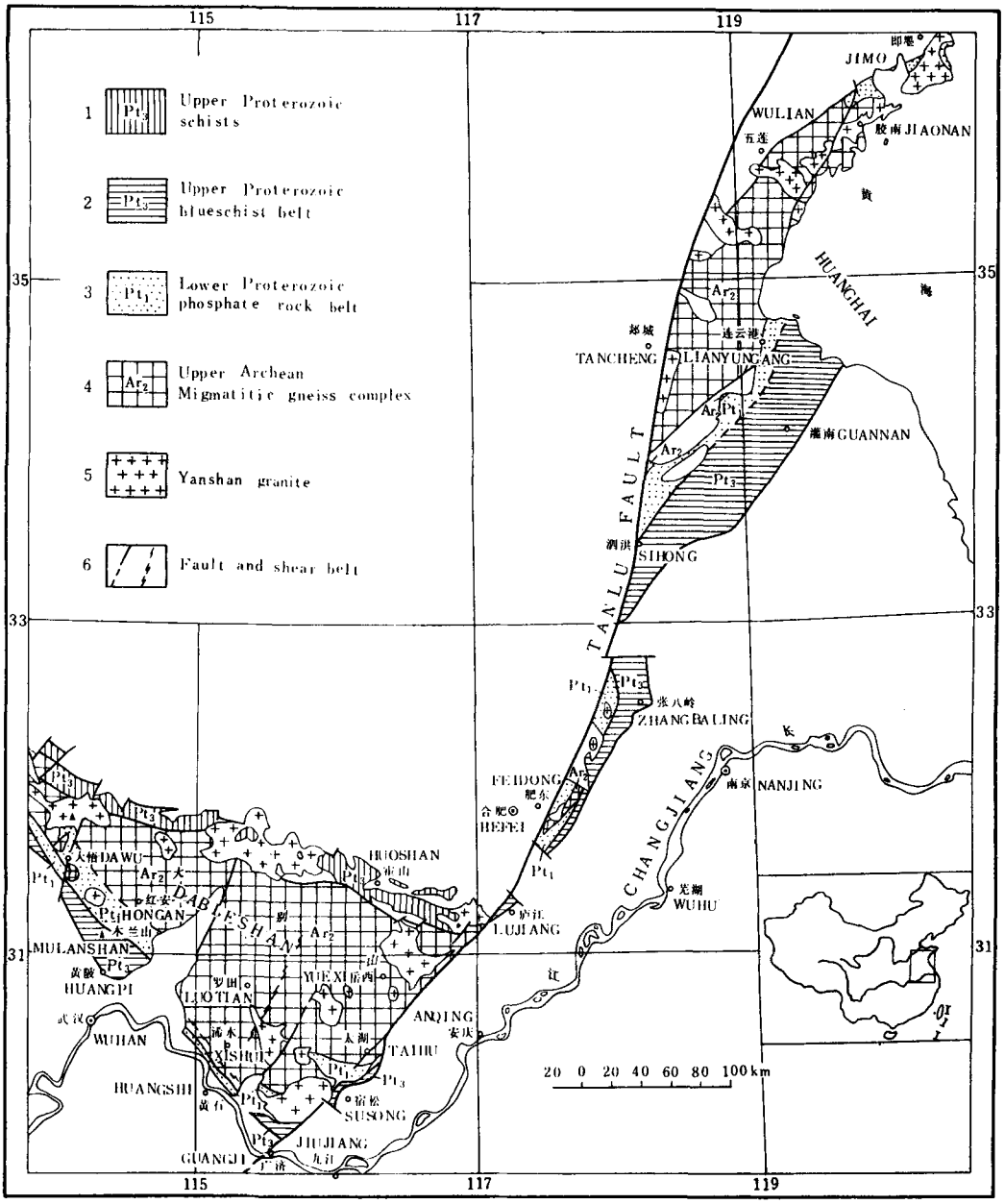

FIG. 1. A schematic geological map of the Dabieshan–Lianyungang area.

apatite extract samples gave an age of 2000 Ma by means of U–Pb isotope dating.* The Lower Proterozoic stratigraphical units are listed in brief as follows:

Upper part: albite gneiss, epidote amphibolite intercalated with quartz mica schist. 1250–2503 m;

* U–Pb isotopes analysed by Yichang Institute of Geology and Mineral Resources, China Academy of Geosciences (1987).

Table 1. The major characteristics of the three suites of Precambrlian metamorphic rocks from the southeastern margin of North China Platform

Meta–strata and isotope dating	Rock association	Metamorphism	Deformation	Ore deposits
Upper Proterozoic. 735 Ma, 848 Ma(Rb–Sr whole rock), 860 Ma (U–Pb whole rock)(1) (fault)	Mainly blueschist, phyllite metamorphic sodium–rich volcanic series	high pressue type greenschist facies regional metamorphism appearance of glaucophane, albite, phengite, stilpnomelane, piemontite and spessartite	highly deformed horizontal shearing: kinks, crenulation cleavage and mylonitization	slight Cu–mine–raliza–tion
Lower Proterozoic. 1850 Ma (zircon U–Pb)(2), 2000 Ma(apatite U–Pb) (unconformity)	meta–sedimentary–volcano –sedimentary rock series comprises: schists, gneiss, leucoleptynite*, epidote amphibolite, marble and phosphorites with ubiqui-tous relic bedding	two–phase metamorphism: primary epidote–amphibolite facies of medium pressure type imposed with secondary retrograde low greenschist facies of low–P–type. migmatization undeveloped	two–phase folding: early macroscopic inclinal folding and later open folds	phos–phor, kyanite
Upper Archaean. 2431 Ma (zircon U–Pb)(3), 2780 Ma (Rb–Sr whole rock)(4)	abundant tonalite–trondhjemite–granodioritic orthogneiss and banded iron ore formation	amphibolite partly granulite facies regional metamorphism and later stage retrograde metamorphism, associated with more than two stages of intensive migmatization	multiphase folding, inten-sive deformation, at least 3–phase folding and tectonic events: tightly closed recumbent folding and intensive foliation transposition(F_1), macro–recumbent–inclinal folding(F_2) and open fold-ing(F_{3+4})(5)	banded iron ore, gold

* leucoleptynite: a metamorphic rock with feldspar > 20, feldspar+quartz > 90(%);
(1) Sang, B. et al.(1987); (2) Anhul Regional Geological Survey; (3) Tao, Q. et al. (1985);
(4) Ying, J. (1988); (5) Suo, S. et al. (1988).

Middle part: leucoleptynite, albite gneiss, epi-dote amphibolite with garneti-ferous green schist intercalated with quartz mica schist, quartzite and kyanite (topaz) schist. 1051–2915 m;

Lower part: marble, quartzite, graphitic schist, quartz mica schist with phosphorite beds. 53–1003 m;

Basal part: muscovite K-feldspar gneiss, K-feldspar quartz mica schist and metaconglomerates. 2–207 m.

Table 2. The chemical composition of the K–rich metamorphic rocks from the basal part of the Lower Proterozoic in Lianyungang area

No.	Sample number	SiO_2	TiO_2	Al_2O_3	Fe_2O_3	FeO	MnO	MgO	CaO	Na_2O	K_2O	P_2O_5	CO_2	H_2O^+	F	LOI	Total
A1	JSZ–1	75.71	0.31	11.86	1.89	0.57	0.02	0.93	0.09	1.54	5.64	0.07				1.60	100.23
A2	H4–2B*	71.16	0.34	13.07	2.62	0.53	0.03	2.17	0.08	1.07	6.10	0.09	0.16	2.25	0.078		99.65
A3	H4–2C*	74.62	0.25	11.41	2.95	0.67	0.02	1.16	0.17	1.60	5.48	0.10	0.15	1.32	0.078		99.98
A4	JS–11	58.61	0.74	14.28	4.09	2.32	2.56	2.83	2.74	0.16	5.41	0.65				4.40	98.79

Nature of samples: A1–A3, muscovite k–feldspar gneiss(A1,A2,matrix from metaconglomerate);A4, K–feldspar quartz mica schist.

*** Sampled by the present author, Analyzed by Testing Lab of the 6th Geological team of Jiansu Province. Other samples are collected from the 6th Geological team.**

This is a sedimentary–volcanosedimentary rock sequence characterized by phosphorite-bearing and aluminous beds, which underwent medium pressure epidote-amphibolite facies regional metamorphism. The relict bedding is ubiquitous, but without any prominent hydrothermal or migmatitic alterations, and is considered to have been isochemical during the metamorphism.

The metasedimentary rock associations of the basal, lower and middle parts

The basal part of the Lower Proterozoic mainly comprises muscovite K-feldspar gneiss and K-feldspar quartz–mica schist (Table 2). Mineralogically they are characterized by significant amounts of K-feldspar and muscovite. The metaconglomerate beds are found in both the Daxinwu–Zhupozhai area of the Anhui–Hubei border and in the Haizhou area of Jiangsu Province. The matrix of these metaconglomerates are also potassium-rich psammites (metamorphosed into muscovite K-feldspar gneiss). Besides, there is always quartzite interbedding; therefore they are K-rich and Si-rich rock associations.

On the [t]–[f] diagram (Fig. 2) the basal potassium-rich rocks are plotted into C_1, C_2 fields, indicating that the nature of the protolith is a differentiated sandstone.

The metaconglomerates are about 3–10 m thick, more than 5–10 km in extent, and have an unconformable contact with the Upper Archaean

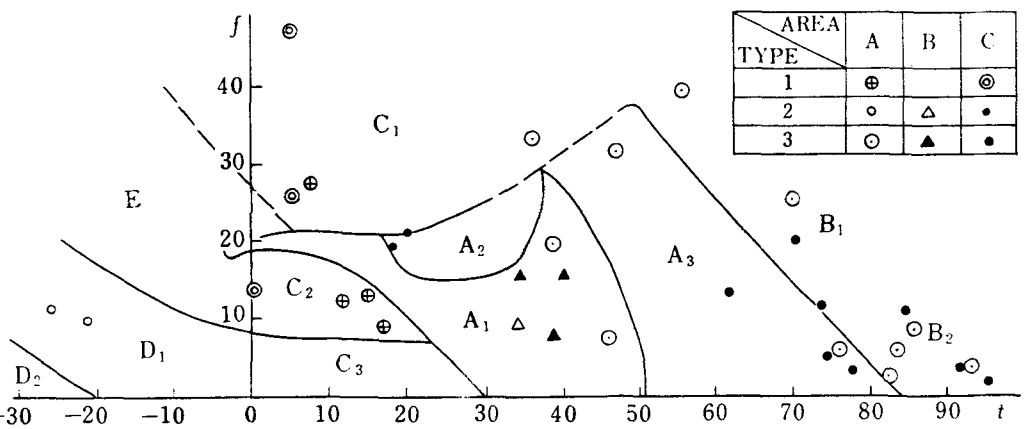

FIG. 2. The [t]–[f] diagram of basal K-rich rocks (1) lower part K-rich rocks (2) and middle part A1-rich rocks (3) of the Lower Proterozoic from Lianyungang (A), Dawu (B) and Susong (C) areas (after Bogdanov *et al.*, 1975). [t], [fm]: Niggli values, [f] = [fm]·[f'],[f'] = ([Fe_2O_3] + [FeO])/([Fe_2O_3] + [FeO] + [MgO]) (mole proportion); Both in diagrams Fig. 6–Fig. 8 and this diagram the chemical compositions of rocks from the Susong are (data from Sand and You, 1988). For the rock analyses of the Lianyungang and Dawu areas see Tables 2–5. Compositional fields see the text.

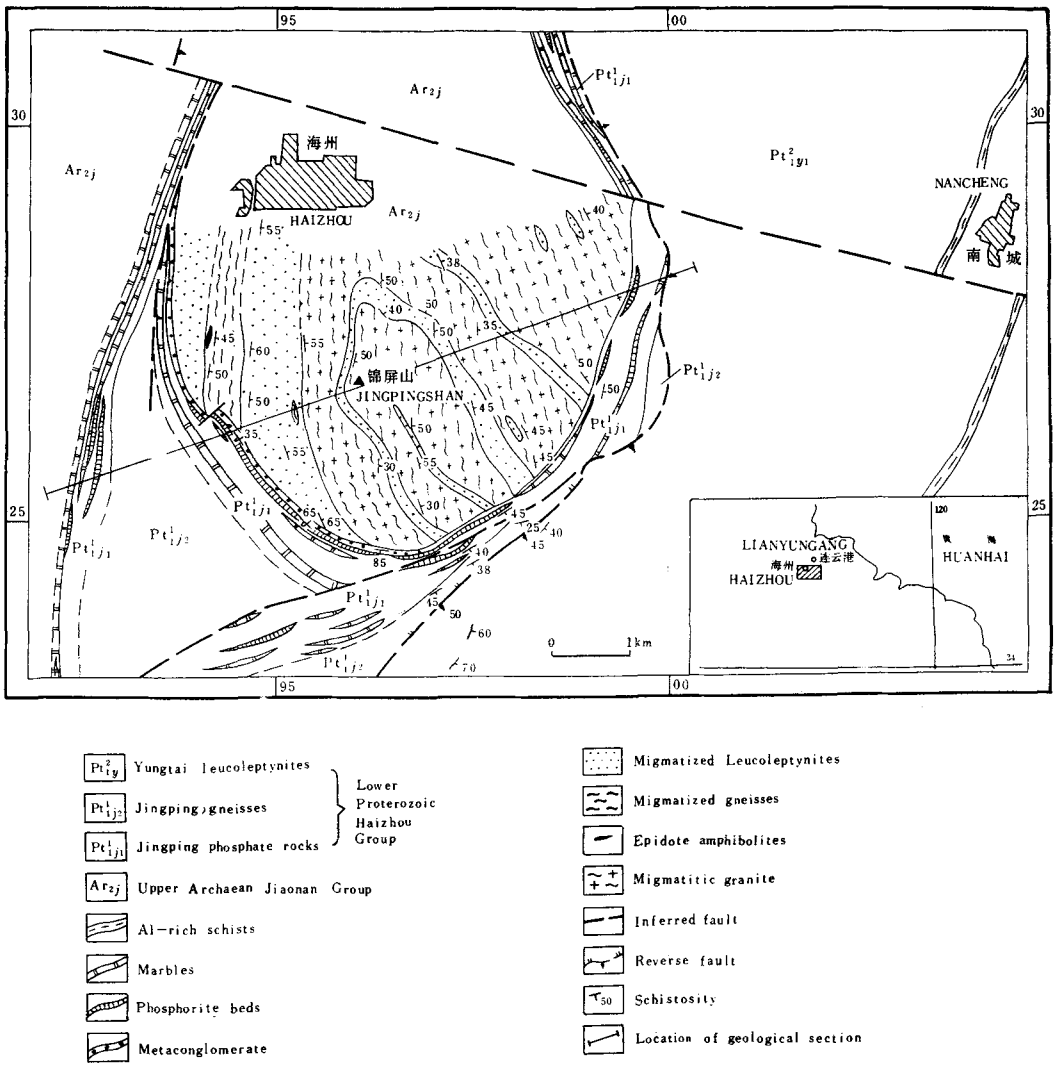

FIG. 3. A geological map of the Haizhou phosphorite mining area, Jiangsu Province.

migmatite complex (Fig. 3, Fig. 4). Pebbles are rounded–subrounded graphic granite, leucoleptynite or quartzite, implying a high textural and compositional maturity. A frequency curve of the distribution of pebble grain size (Fig. 5), showing a single maximum, indicates the seashore environment. From the features mentioned above, these metaconglomerates are seashore basal conglomerates, indicating a long sedimentary gap before their deposition.

Consequently, the basal K-rich and Si-rich rock associations of the Lower Proterozoic represent a suite of protoliths of terrigenous clastic nature comprising the highly matured quartzose sandstone, quartzo-feldspathic sandstone and conglomerate, the high textural and compositional maturity implying the stability of the tectonic environment during their formation.

In the lower part of the Lower Proterozoic, various kinds of marble and calcareous mica-schist are developed (Table 3, Fig. 3). These rocks are rich in calcium, mineralogically abundant with carbonate and calc–silicate minerals, and are derived from calcareous sedimentary protoliths. Associated with these calcium-rich rocks are phosphorite, quartzites, graphite-

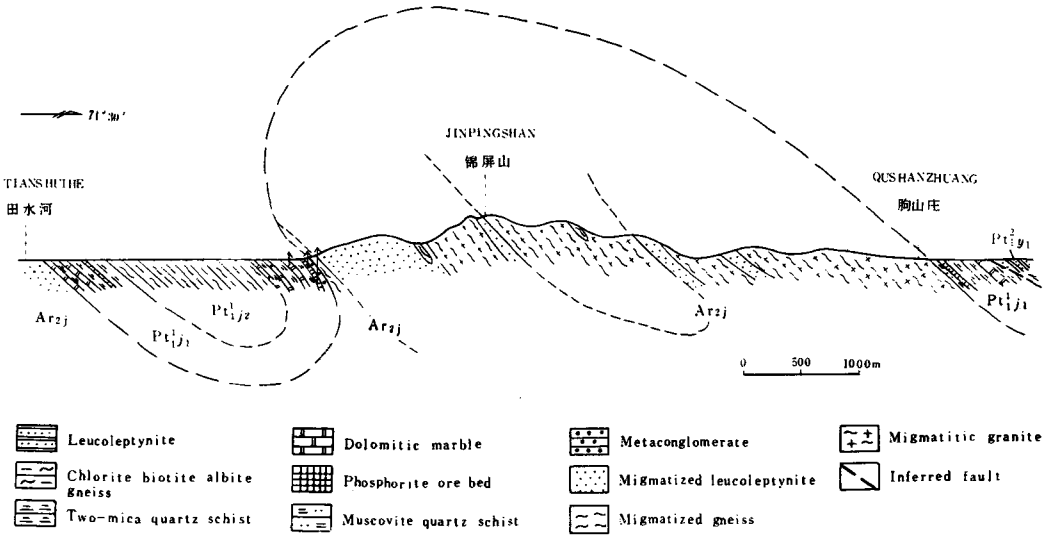

FIG. 4. The geological section through Jingpingshan. The location of this section see Fig. 3.

bearing mica-schist and K-feldspar quartz mica-schists, forming a suite of phosphorus–silica-rich carbonaceous–potassium-rich rocks in which the well-known meta-phosphorite deposits of Haizhou Jiangsu, Susong Anhui and Dawu Hubei are formed. The potassium-rich rocks in this suite, in contrast to those of the basal part, are lower in SiO_2. On the [t]–[f] diagram (Fig. 2) they plot in the A1, A2, and D1 fields. The protoliths are hydromica pelites and sandstone with carbonate impurities.

Consequently, the protolith of the lower part of the Lower Proterozoic is a phosphoritic formation composed of phosporite, chert, dolomite, limestone, carbonaceous shale, calcareous sandstone and hydromica pelite. This protolith association is completely correspondent with the phosphoritic formation of ocean current origin (Sang and You, 1988), suggesting that they were formed under a shallow marine environment of an ancient continental margin. A stable tectonic setting is favoured for the formation of the phosphorous deposits.

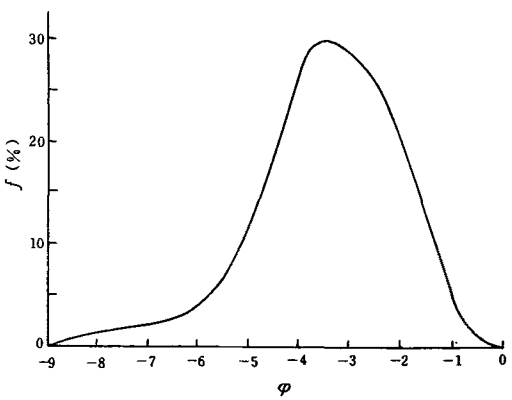

FIG. 5. The frequency curve of the distribution of pebble grain size in the Haizhou metaconglomerate, based on 468 measurements.

In the middle of the Lower Proterozoic, a suite of quartzite, mica quartz schist and kyanite (topaz) schist, chloritoid schist, kyanite (topaz) quartz schists (about 35–600 m in thickness) is widely developed (Table 4, Fig. 3), in which the kyanite ore deposits in Hanshan Jiangsu and Qingshuitang Anhui occur. The quartzite and mica–quartz schist have a high silica content, $SiO_2 > 80$ (wt.%), while others are aluminous, mineralogically characterized by the occurrence of Al_2SiO_5 minerals, chloritoid, corundum and other aluminosilicates. On the [t]-[f] diagram (Fig. 2), they plot in the B1, B2 and A1, A3 fields, indicating that the protoliths are bauxites, kaolinite pelites and well-differentiated pelitic rocks. Therefore this Si-rich–Al-rich rock association is an alumino–siliceous sedimentary formation formed on the stabilized continental margin.

The metavolcanic-sedimentary rock association of the mid and upper parts

The mid and upper parts of the Lower Proterozoic are mainly composed of muscovite–

Table 3.The chemical composition of the phosphoritic formation from the lower part of the Lower Proterozoic

Area	Chemical type	No.	Sample number	SiO_2	TiO_2	Al_2O_3	Fe_2O_3	FeO	MnO	MgO	CaO	Na_2O	K_2O	P_2O_5	CO_2	H_2O^+	F	LOI	Total
Lianyungang	P-rich	A5	JS-28	7.06	0.09	1.34	1.13	0.34	0.48	7.17	41.96	0.14	0.39	21.62	16.64	0.57	1.69		100.62
		A6	JS-29	24.93	0.22	5.64	4.65	0.43	1.62	2.93	29.71	0.08	1.78	15.35	8.52	0.70	1.24		97.71
		A7	JS-30	24.92	0.05	1.98	8.74		10.80	5.45	25.59			18.17	0.61		1.61		97.92
	Mn-rich	A8	W350-6*	12.75	0.36	1.26	5.43	0.47	32.50	3.04	15.58	0.10	0.10	1.32	27.09	1.12	0.136		101.26
		A9	W350-5A*	18.27	0.60	3.22	4.97	1.89	20.84	3.54	15.98	1.84	0.53	2.50	24.37	1.47	0.272		100.27
	Carbonaceous	A10	JS-9	54.56	0.71	15.65	2.88	1.79	1.22	2.49	3.68	0.76	7.67	2.22				6.01	99.64
	Si-rich	A11	JS-7	97.68		0.21	0.64		0.02	0.20	0.71			0.09				0.25	99.80
	Ca-rich	A12	W350-2*	2.74	0.06	0.87		0.90	0.92	19.45	29.44	0.02	0.39	0.19	43.46	1.06	0.056		99.56
		A13	W350-7*	1.94	0.06	0.50	0.16	0.25	0.71	21.28	29.78	0.02	0.15	0.08	45.28	0.85	0.042		101.10
		A14	JS-3	11.36	0.40	2.48	5.09	0.83	2.10	15.74	24.81	0.10	1.43	0.41	32.40	0.14			97.29
		A15	JS-4	21.78	0.52	4.18	1.87	1.32	0.21	11.51	25.49	0.12	1.82	0.20	30.66	0.26			99.94
		A16	JS-6	28.04	0.50	5.41	2.00	1.20	0.10	9.72	23.32	1.37	0.70	0.19				27.13	99.48
		A17	E350-4*	28.38	0.59	5.33	1.76	2.57	0.13	12.24	20.42	0.08	1.74	0.18	24.01	2.52	0.196		100.15
		A18	JS-5	13.48	0.27	2.37	1.15	1.21	0.03	15.65	27.55	0.68	0.40	0.13				36.42	99.34
	K-rich	A19	JS-12	57.16	0.58	12.21	1.28	1.00	0.87	2.59	7.06	0.06	8.00	2.76	3.93	2.13			99.63
		A20	JS-10	43.00	0.84	8.02	3.50	2.00	0.18	10.35	10.75	0.06	5.00	0.35	13.97	0.62			99.64
Dawu	P-rich	B1	23-2*	45.14	0.32	6.60	0.51	0.59	0.04	0.72	22.70	0.10	3.89	17.50	0.10	0.75		1.21	99.80
		B2	23-5*	59.16	0.29	6.11	1.59	0.10	0.06	0.37	15.22	0.12	4.23	11.20	0.07	0.70		0.78	99.77
	Carbonaceous	B3	23-4*	79.04	0.48	7.48	3.54	0.16	0.01	0.45	0.09	0.10	4.42	1.23	0.07	1.63	0.10	2.98	100.00
		B4	7-1*	74.23	0.53	11.36	3.49	0.55	0.02	1.42	0.03	0.17	3.94	0.04	0.14	1.97	0.18	3.80	99.64
	Si-rich	B5	7-2*	91.33	0.41	4.19	1.50	0.39	0.02	0.11	0.09	0.38	0.26	0.02	0.10	1.25	0.01		100.16
	Ca-rich	B6	1108-BU	3.26	0.04	0.40	0.64		0.05	20.32	29.48	0.24		0.01		0.64			55.08
		B7	1748-19	17.78	0.06	0.87	1.22		0.03	17.43	23.61			0.01					61.01
		B8	1720-35	14.51	0.03	0.24	0.23		0.03	17.55	27.06			0.01					59.66
		B9	2357-10	11.70	0.25	3.98	1.66	3.62	0.15	13.82	29.42	0.25	0.08	0.05		2.38			67.36
		B10	1719-32	35.59	0.03	0.04	0.41		0.03	14.96	18.61			0.07					69.74
	K-rich	B11	23-3*	73.70	0.35	14.60	1.09	0.58	0.02	0.73	0.06	0.12	5.38	0.05	0.06	2.10	0.07	2.54	99.28

Rock names: A5–A7,B1,B2, phosphorite; A8,A9, rhodochrosite marble; A10, graphitic muscovite schist;B3,B4,graphitic muscovite quartz schist, totals include C: 0.72(B3),1.22(B4); A11,B5, quartzite; A12–A14, B6–B8, dolomitic marble; A15–A17,B10, mica quartz marble; A18,B9, tremolite marble; B11, K-feldspar muscovite quartz schist; A19, K-feldspar muscovite schist; A20, two mica schist.

* Samples collected by the author, analyst: Testing Lab of the 6th Geological team of Jiangsu Province (for samples from Lianyungang) and Chemical Lab of China University of Geosciences (for Dawu samples). Other samples are from the 6th Geological team of Jiangsu Province (for Lianyungang samples) and Regional Geological Survey party of Hubei Province (for Dawu samples).

Table 4. The chemical composition of the alumino–siliceous formation from the mid of the Lower Proterozoic

Area	Chemical type	No.	Sample number	SiO_2	TiO_2	Al_2O_3	Fe_2O_3	FeO	MnO	MgO	CaO	Na_2O	K_2O	P_2O_5	CO_2	H_2O^+	F	LOI	Total
Liuyang		A21	ZK402–1	96.28	0.77	1.47	0.24	0.79	0.01		0.28		0.26	0.06				0.15	100.31
	Si–rich	A22	HK8–4*	96.10	1.18	0.51	1.12	0.10			0.55	0.05	0.05	0.02	0.11	0.15	0.032		99.97
		A23	D101–1	80.54	0.38	10.24	2.03	0.62	0.01	0.29	0.16	0.07	2.74	0.25				2.63	99.96
		A24	Y7–5*	38.02	2.11	34.30	2.56	11.1	60.42	1.65	0.06	0.77	3.12	0.16	0.05	5.56	0.126		99.98
		A25	Y7–2*	48.44	0.33	44.80	0.58	0.23	0.02	0.33	0.20	0.75	1.71	0.04	0.07	1.75	0.078		99.33
		A26	HK9–3*	54.36	1.93	30.17	8.19	0.10		0.04	0.46	0.05	0.02	0.47	0.05	5.26	1.00		101.58
		A27	HK15*	60.06	1.15	16.72	8.12	0.23			0.43	0.48	3.25	0.30	0.20	9.00	0.124		100.06
		A28	HK9–1*	64.56	0.03	27.89	0.02	0.72			0.20	0.04	0.01		0.08	6.12	0.115		99.79
	Al–rich	A29	Y7–1	64.68	0.37	29.70	0.59	1.47	0.04	0.03	0.23	0.10	0.30	0.10	0.16	1.79	0.061		99.62
		A30	HK6*	67.58	0.44	18.20	4.44	0.30		0.26	0.15	0.63	4.51	0.08	0.05	4.39	0.130		101.16
		A31	HK2*	72.20	1.20	16.16	8.37	0.23			0.29	0.06	0.02	0.05	0.12	2.57	0.026		101.30
		A32	HK8–3*	79.56	1.13	16.82	0.61	0.26		0.05	0.38	0.09	0.10	0.29	0.05	0.42	0.156		99.92
		A33	TC1601	76.80	0.99	16.39	0.39	0.50	0.01	0.21	0.72	0.10	0.00	1.00				2.43	99.54
		A34	HK8–2*	77.00	1.41	14.60	0.90	0.09		0.14	0.26	0.45	3.19	0.26	0.05	1.99	1.20		100.46
Dawu		B12	1377–1	79.21	0.31	12.35	1.86	0.65	0.01	0.36	0.14	1.28	2.38	0.19		1.89			99.63
	Al–rich	B13	2357–15	73.21	0.25	16.63	1.04	0.52	0.01	0.68	0.30	1.80	2.65	0.09		2.46			99.64
		B14	Q11	77.16	0.53	13.25	1.53	0.97	0.02	0.38	0.21	1.20	1.93	0.09		2.28			99.55

Rock names:A21,A22, quartzite; A23,B12–B14, muscovite quartz schist; A24, chloritoid schist; A25, A26, A28, pyrophyllitized kyanite schist; A27, topaz quartz schist; A29, chloritoid kyanite quartz micaschist; A30,A34, kyanite quartz micaschist; A31,kyanite quartz schist; A32, topaz andalusite kyanite quarz schist; A33, kyanite topaz quartz schist.

*** The same as in Table 3**

albite gneiss, two-mica albite gneiss, epidote amphibolite, garnet-bearing greenschist, leucoleptynite, and K-feldspar mica-schist (Table 5). Except for the leucoleptynite and K-feldspar mica-schist, the rocks are chemically neither Ca-rich, Al-rich, nor K-rich. Mineralogically there is a lack of carbonates, aluminosilicates and K-feldspar. It is a corollary that they are compositionally 'normal' rocks.

On the Al–K–Na diagram (Fig. 6) this suite of normal rocks and K-rich rock associations is partly plotted in the sedimentary sector field (SSF) and its boundaries; therefore they are sedimentary-derived paragneisses (the numbered plots on the diagram). But, the majority of the samples are plotted in the Pacific type calc–alkaline field (CAP) and in the intermediate volcanic rock field (INT). If these metavolcanics are plotted on the K_2O–SiO_2 diagram (Fig. 7), most of them plot in the calc–alkaline rock series (C), including high-alumina basalt (4), andesite (5), dacite (6) and rhyolite (7).

In Table 6 the results of the trace element analyses for the metabasites from the Susong and Dawu areas are indicated. No. 50 from Susong and No. B22 from Dawu are parametabasites (Fig. 6); others are derived from basaltic rocks.

The trace-element characteristics are different in basalts from various tectonic settings. The convenient means of comparing analyses for these various magma types is to plot the data as geochemical patterns (Pearce, 1982). The geochemical patterns of the three metabasalts from Susong and Dawu (Fig. 8, samples B28, 52, 53) show high enrichment of Rb, Ba and Th and associated enrichment of Ce, P, Sm and Ti; this is very similar to the patterns typical for continental volcanic arc calc–alkaline basalts. It can be seen from Fig. 8 that the patterns of the two parabasite samples show similar features to those basalts

Table 5. The chemical composition of the metavolcano–sedimentary rocks from the middle and upper part of the Lower Proterozoic

Area	Chemical type	No.	Sample number	SiO_2	TiO_2	AL_2O_3	Fe_2O_3	FeO	MnO	MgO	CaO	Na_2O	K_2O	P_2O_5	CO_2	H_2O^+	F	LOI	Total
Liaoyuanzi	K-rich	A35	JS-8	77.02	0.10	11.17	0.86	0.65	0.13		0.42	1.58	5.44	0.04	0.44	0.84			98.69
		A36	ZK001	75.54	0.30	11.67	1.87	0.80	0.03	0.61	0.15	3.83	4.68	0.03				0.55	100.06
	Normal	A37	ZK001-4	75.48	0.29	13.12	1.95	2.15	0.03	0.45	0.12	0.20	3.60	0.16				2.15	99.70
		A38	ZK001-5	67.60	0.37	18.36	1.92	1.20	0.03	0.55	0.10	0.11	5.10	0.28				3.73	99.35
		A39	ZK001-1	66.08	0.64	16.89	2.55	1.19	0.03	1.38	0.09	4.22	4.04	0.12				2.30	99.53
		A40	ZK001-3	74.18	0.20	15.11	0.66	1.55	0.03	0.94	0.16	4.09	2.76	0.12				0.83	100.63
		A41	ZK805-2	70.82	0.40	15.78	1.50	0.77	0.04	0.43	0.13	5.00	4.16	0.12				1.01	100.16
		A42	ZK402-3	69.50	0.51	15.91	2.32	1.02	0.01	0.71		4.00	3.84	0.08				1.96	99.86
		A43	HK4*	68.96	0.52	15.40	2.43	0.85	0.04	0.69	0.27	4.59	3.72	0.23	0.05	1.62	0.062		99.43
		A44	JS-13	73.74	0.03	12.50	0.56	1.20	0.08	1.44	1.63	2.64	3.09	0.12				3.12	100.15
		A45	JS-24	70.48	0.23	14.28	1.23	2.37	0.08	0.55	1.11	3.28	4.45	0.09				1.44	99.59
		A46	JS-25	68.54	0.25	14.73	1.50	1.43	0.09	0.73	1.51	3.45	4.46	0.10				2.88	99.67
		A47	JS-14	65.00	0.38	15.71	1.01	3.43	0.14	1.74	3.07	2.46	3.39	0.18				2.98	99.49
		A48	E350-7*	63.36	0.54	13.89	2.71	2.80	0.28	3.36	4.29	2.84	2.36	0.21	0.78	1.91	0.122		99.45
		A49	JS-18	59.40	0.67	14.38	1.36	5.54	0.16	3.25	4.74	2.92	2.70	0.28				3.99	99.12
		A50	JS-16	56.88	0.78	18.26	5.28	2.17	0.11	2.19	6.37	3.36	2.63	0.37	0.76	0.98			100.14
		A51	JS-15	56.92	0.33	16.97	2.27	4.31	0.15	3.67	5.61	3.95	1.96	0.27				2.67	99.08
		A52	E350-2*	48.82	0.82	16.87	4.65	5.17	0.24	7.80	7.13	2.64	1.84	0.29	0.27	2.78	0.075		99.40
		A53	JS-20	49.58	0.93	16.00	4.87	4.80	0.17	6.21	8.43	3.08	2.06	0.26	1.22	1.73			99.34
		A54	JS-21	50.10	0.91	16.64	4.98	5.14	0.09	6.47	8.76	3.38	0.59	0.24				2.37	99.67
		A55	JS-23	48.84	1.19	18.58	3.53	6.38	0.27	4.13	7.96	3.51	1.54	0.36				3.27	99.56
Dawa	K-rich	B15	13-2*	75.86	0.09	11.26	1.32	0.68	0.09	0.33	0.32	0.79	8.38	0.07	0.10	0.69			99.98
		B16	Q4	76.10	0.23	10.41	1.90	1.24	0.03	0.12		4.38	4.42	0.07		0.58			99.48
		B17	726-136	77.30	0.18	11.40	1.64	0.67	0.18		0.41	3.57	4.48			0.63			100.46
	Normal	B18	Q1008-1	70.27	0.31	13.82	1.82	1.87	0.03	0.45	5.19	1.00	2.24	0.04		2.19			99.23
		B19	9-1*	75.43	0.25	13.15	1.37	0.32	0.06	0.23	0.64	3.14	3.61	0.04	0.13	1.05	0.02		99.67
		B20	2351-1	72.97	0.38	13.53	1.81	1.38	0.03	0.61	0.14	4.25	3.76	0.10		1.21			100.17
		B21	1096-48	54.83	2.09	12.19	4.77	7.73	0.18	3.20	10.78	1.67	0.22	0.40		1.56		1.32	99.62
		B22	8-2*	48.42	0.89	18.50	2.60	6.91	0.15	5.80	11.44	2.59	0.26	0.06	0.08	1.09	0.02		99.71
		B23	Q16	47.60	2.90	14.50	6.22	8.62	0.27	5.39	8.40	2.88	0.27	0.61		2.26			99.62
	Normal	B24	2001-39	47.55	1.50	16.30	4.42	7.66	0.20	7.79	0.60	3.28	0.23	0.25		2.20			91.98
		B25	1889-75	49.01	2.95	12.09	3.63	11.83	0.33	4.49	9.40	2.10	0.30	1.42		1.79			99.34
		B26	2703-1	48.10	1.63	16.15	3.02	8.26	0.18	7.65	9.38	2.68	1.00	0.15		2.46			100.66
		B27	2021-45	47.60	3.10	12.97	3.78	12.01	0.26	6.00	9.23	2.48	0.35	0.38		0.35			99.51
		B28	12-1*	45.44	3.24	12.14	7.33	10.17	0.23	5.19	9.60	3.30	0.41	0.37	0.14	1.70	0.03		99.29
		B29	6-1*	42.92	0.02	1.06	1.26	4.96	0.07	37.86	0.04	0.02	0.02	0.00	0.11	11.72	0.04		100.10
		B30	6-3*	37.87	1.85	16.74	4.26	9.24	0.25	11.35	12.35	0.48	0.20	0.16	0.12	5.30			100.17

Rock names: A35,A36,B15–B17, leucoleptynite; A37,A38, muscovite quartz schist; A39–A46, B18–B20, muscovite albite gneiss; A47–A51,B21, epidote two–mica albite gneiss; A52–A54, B26–B28, albite epidote amphibolite ; A55, garnet greenschist; B22,B25, garnet epidote amphibolite; B23,B24, quartz epidote amphibolite; B29,serpentine; B30,chlorite schist.

* The same as in Table 3.

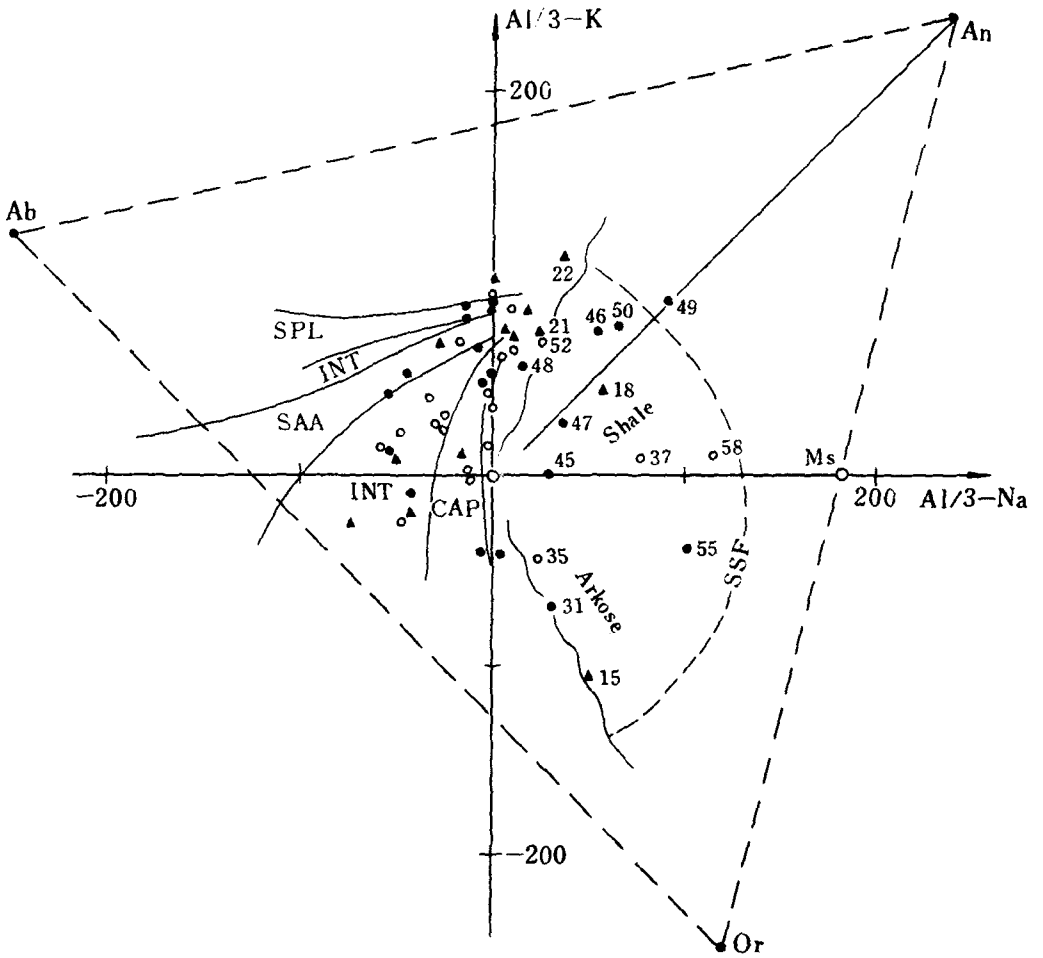

FIG. 6. The compositional plots of the normal and K-rich rocks from the mid–upper part of the Lower Proterozoic on the Al–K–Na diagram. After de La Roche (1968) simplified, quoted from You *et al.* (1986). The solid dots, triangles and open circles—samples from Susong, Lianyungang and Dawu areas respectively. SPL, spilites; SAA, sodium-alkaline Atlantic volcanism; CAP, calcalkaline Pacific volcanism; INT, intermediate volcanic rocks; SSF, sedimentary sector field.

mentioned above (with high enrichment of Rb, Ba and Th), but their prominant depletion of Zr, Hf, Sm, Ti, Y and Yb is obviously different from them. It is presumed that the protoliths of these parabasites are basic pyroclastic sedimentary rocks. The addition of the sediments caused the abundance of immobile elements such as Zr and Yb to significantly decrease without changing the abundance of Rb, Ba and Th.

From Table 6, it can be seen that for the three metabasite samples, ΣREE = 121.66–162.03 p.p.m., $(Ce/Yb)_N$ = 2.03–2.38, ΣREE and $(Ce/Yb)_N$ are increased as the SiO_2 content increases. Eu/Eu* = 0.99–1.05 without a Eu anomaly. The normalized *REE* distribution patterns (Fig. 9) decrease uniformly from La to Lu. The trends of the three curves are almost parallel. These characteristics are coincident with those of tholeiite (*senso lato*) patterns from both island arc and back-arc basin (Cullers and Graf, 1984). While the two parabasites show similar *REE* patterns to those basalts mentioned, but ΣREE is significantly lower (ΣREE = 57.30 and 44.73 p.p.m. respectively), which also indicates that the protoliths were presumably basic pyroclastic rocks. The addition of the sediments has diluted the *REE* content.

On the Th/Yb–Ta/Yb diagram (Fig. 10*a*) these

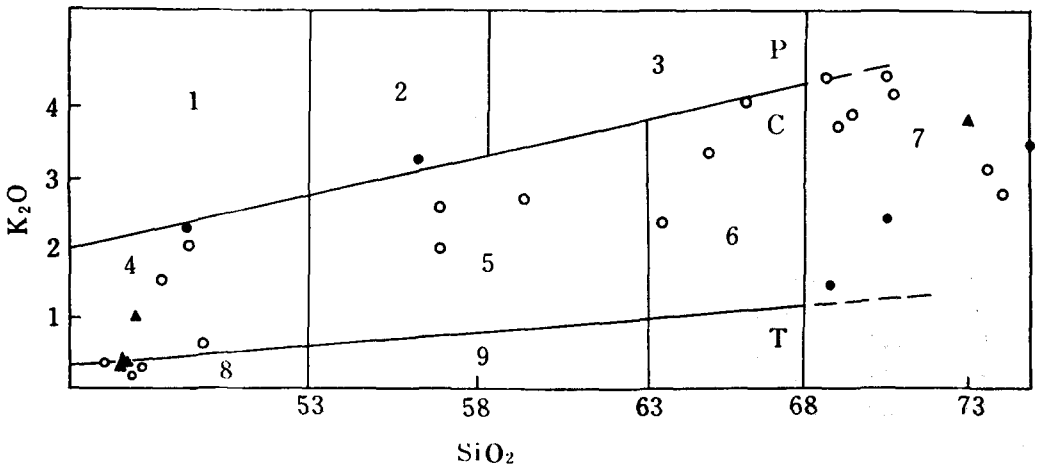

FIG. 7. K_2O–SiO_2 (wt.%) diagram for the Lower Proterozoic metavolcanic rocks. After Barberi (1974) quoted from Boillot (1981). Symbols see Fig. 6. T, tholeiitic series; C, calc–alkaline series; P, potassium series; 1, shoshonitic and alkaline basalts; 2, latites, hawaiites; 3, trachytes; 4, high-alumina basalts; 5, andesites; 6, dacites; 7, rhyolites; 8, tholeiites; 9, icelandites.

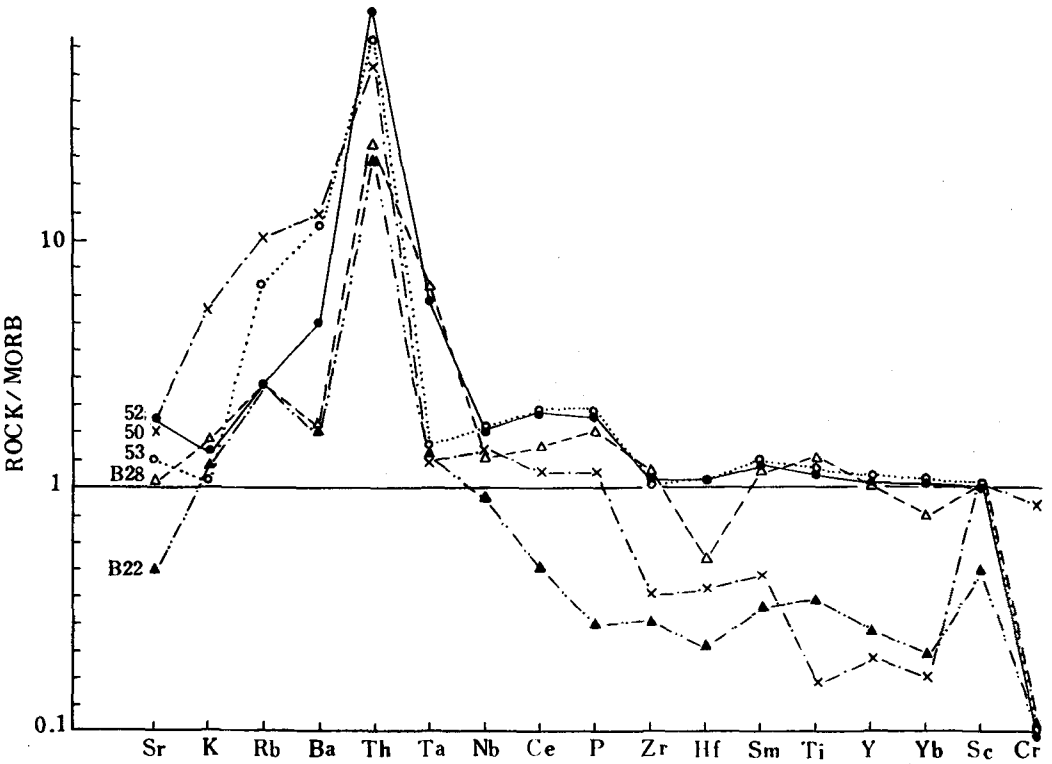

FIG. 8. Geochemical patterns of the Lower Proterozoic metabasites. The numbers in the diagram indicate the analyses shown as in Table 6.

Table 6. Trace element analyses for the metabasites from Susong and Dawu areas (ppm)

Area	Susong			Dawu		Area	Susong			Dawu	
No.	50	52	53	B22	B28	No.	50	52	53	B22	B28
La	7.86	15.7	16.9	3.99	10.63	Eu / Eu*	0.99	0.99	1.04	1.11	1.05
Ce	16.1	37.5	37.9	7.08	25.22	Sc	43.7	41.0	42.3	28.0	46.9
Pr	2.52	5.42	5.76	1.35	4.02	Ti	2148	15221	17366	4590	14743
Nd	8.83	22.5	24.1	6.38	19.72	V	148.0	522.0	509.0	280.3	718.2
Sm	2.29	6.02	6.52	1.81	5.16	Cr	232	33.1	22.1	32.8	28.2
Eu	0.73	2.04	2.33	0.73	1.87	Co	42.5	54.4	62.8	41.7	57.5
Gd	2.20	6.70	7.23	2.29	5.82	Ni	124	20.6	5	66.3	31.0
Tb	0.46	1.23	1.34	0.40	0.97	Cu	15.7	138.0	20.7	181.2	97.6
Dy	2.21	7.17	7.75	2.45	6.16	U	0.49	1.13	1.13	0.52	1.34
Ho	0.44	1.47	1.59	0.53	1.25	Th	14.7	18.8	16.6	7.7	9.0
Er	1.22	4.22	4.54	1.51	3.58	Nb	8.2	11.0	11.2	3.4	7.5
Tm	0.23	0.68	0.74	0.23	0.53	Ta	0.38	1.40	0.47	0.40	1.5
Yb	1.05	4.03	4.27	1.34	3.08	Zr	54.6	117.0	105.0	46.0	148.0
Lu	0.16	0.61	0.66	0.19	0.45	Hf	1.50	3.18	3.12	1.00	1.78
Y	11.0	36.8	40.4	14.45	33.20	Rb	22.4	9.4	16.7	9.4	9.4
$\sum$REE	57.30	152.09	162.03	44.73	121.66	Sr	410.0	415.0	234.0	84.0	138.0
$(Ce/Yb)_N$	3.90	2.38	2.26	1.35	2.09	Ba	404	137	298	61	64
SiO_2	48.60	47.13	47.80	48.42	45.44	K_2O	1.13	0.33	0.18	0.26	0.41

No.50 of Susong & No.B22 of Dawu are parametabasites, others are metabasalts. The relevant chemical analyses see Table 5 in the present paper & Table 2 of Sang et al.(1988). Here only SiO_2 & K_2O(Wt%) are indicated.

Analyst: The Geological Lab of Hubei Province. Methods: XRF for Cr, Th,Nb,Zr,Rb; ICP for others.

basic metamorphic volcanics and pyroclastics are plotted in the SHO field and on the boundary between the SHO and CAB fields. On the Th–Hf–Ta diagram (Fig. 10*b*) they are plotted in the CAB field.

Consequently, the middle and upper part of the Lower Proterozoic is a suite of metamorphic rocks composed of basalt–andesite–rhyolite and a small amount of low-maturity clastic sedimentary rocks. The calc–alkaline volcano–sedimentary formation and its chemical features indicate that during the mid–late period of the early Proterozoic this area was in an active continental margin tectonic setting.

The Proterozoic tectonic evolution

In conclusion, the study of the rock association and chemical characteristics of the Lower Proterozoic metamorphic strata indicates that the basal and lower parts of the metastrata is a rock association composed of terrigenous clastics and phosphoritic formation of a miogeosynclinal environment, which provides evidence that this area belonged to a stabilized continental margin during the earlier period of the early Proterozoic (see Fig. 11). Also, the Si-rich and Al-rich sedimentary formations in the middle part of the Lower Proterozoic show the characteristics of a stabilized continental margin. The middle–upper parts are calc–alkaline volcano–sedimentary formations formed at the active continental margin. All of these indicate that during the mid–late period of the early Proterozoic the convergence of the Yangtze and North China plates began along the stabilized continental margin characterized by miogeosynclinal deposits. The entire metasedimentary–volcanosedimentary rock sequence of the Lower Proterozoic suggests that

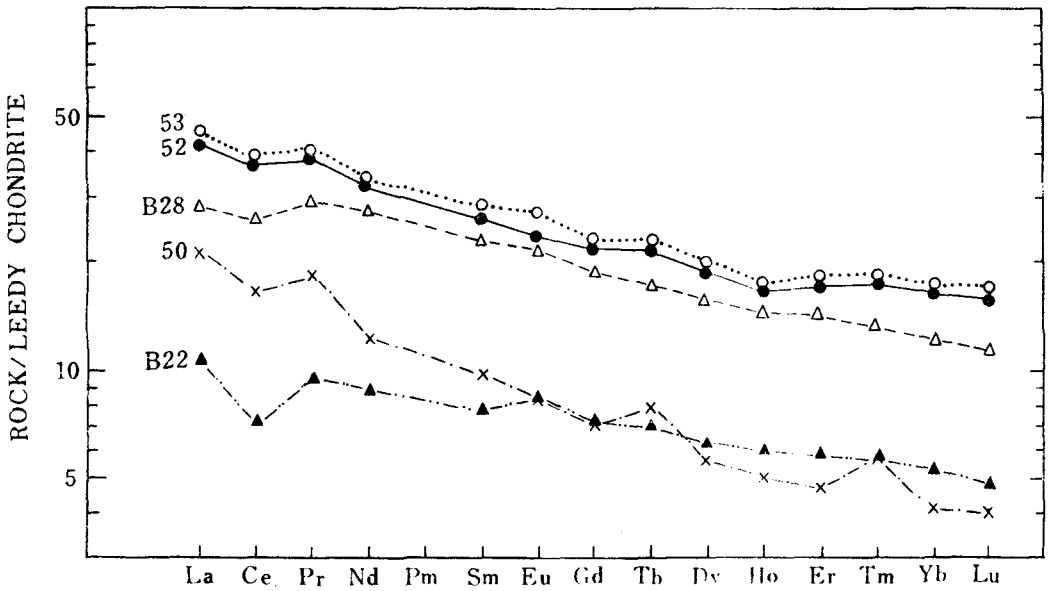

FIG. 9. *REE* distribution patterns of the Lower Proterozoic basic metamorphic rocks. The numbers in the graph see Table 6.

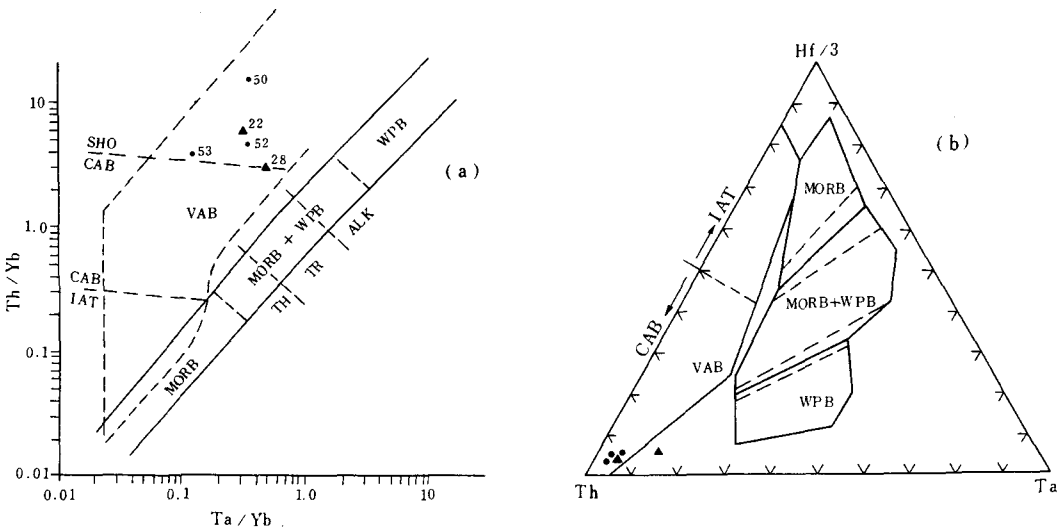

FIG. 10. The Th/Yb–Ta/Yb diagram (*a*, after Pearce, 1982) and the Th–Hf–Ta diagram (*b*, after Wood, 1980) for the Lower Proterozoic metabasic volcanics and pyroclastics from the Susong (solid dots) and Dawu (solid triangles) areas. The numbers in the graph see Table 6. VAB, volcanic arc basalt, including island arc tholeiite (IAT); calc–alkaline basalt (CAB); and shoshonite (SHO); MORB, mid-ocean ridge basalt; WPB, within-plate basalt. Both MORB and WPB include tholeiitic (TH), transitional (TR) and alkalic (ALK).

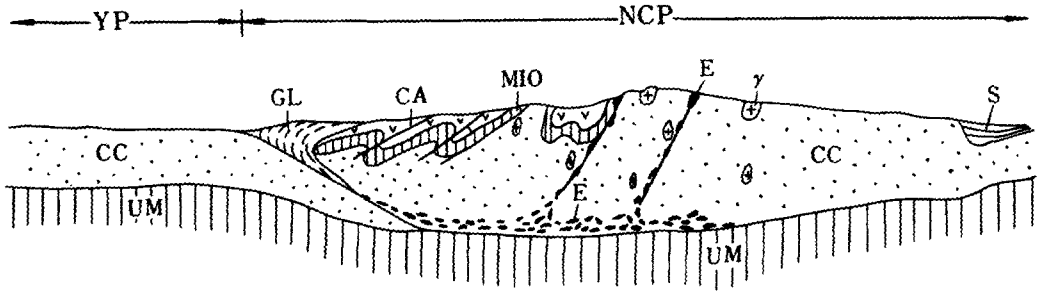

FIG. 11. A schemetic tectonic section through the Precambrian of Dabieshan. YP, Yangtze Plate; NCP, North China Plate; CC, continental crust; UM, upper mantle; GL, glaucophane green schist; S, schist; CA, calc-alkaline volcanic rocks; MIO, miogeosyncline deposits; E, eclogite; γ, granitoids.

throughout the early Proterozoic there was a process of tectonic evolution from stabilization to mobilization.

In the late Proterozoic blueschist belts, flanking the south of the Lower Proterozoic, there is a spilite–keratophyre formation. To the north of the Lower Proterozoic there is also an eclogitic belt parallel with the blueschist belt (Dong *et al.*, 1986). The eclogitic bodies tectonically emplaced in the Lower Proterozoic, near the boundary between Lower Proterozoic and Upper Archaean and in the Upper Archaean gneiss–migmatite complex, indicate that the convergence process came to a peak during the later Proterozoic time which finally resulted in the collision and amalgamation of the Yangtze old land and North China old land.

Acknowledgements

The present paper is completed with the financial support of the National Scientific Foundation (NSF No. 85040093), the guidance of Prof. You Zhendong, and the friendly support of Prof. Sun Dazhong, to whom the author wishes to convey his deep gratitude.

References

Bogdanov, U. B., Voinov, A. S., Efron, A. S. (1975) Some geochemical characteristics of the metamorphic strata of the Chupa–Loukhi area. In *Problems of Magmatism and Metamorphism*, Vol. V (Editor-in-chief T. V. Perekalina; in Russian). Leningrad University Press, Leningrad, 31–40.

Boillot, G. (1981) *Geology of the Continental Margins* (English translation, translated by A. Scarth). London & New York, 81.

Cullers, R. L. and Graf, J. L. (1984) Rare earth elements in igneous rocks of the continental crust: In *Rare Earth Element Geochemistry* (P. Henderson, ed.) Elsevier, Amsterdam, 237–68.

Dong, S. *et al.* (1986) Metamorphism in China and its Relation with the Crustal Evolution (in Chinese). *Geological memoirs*, Series 3, No. 4, Geological Publishing House, Beijing.

Pearce, J. A. (1982) Trace element characteristics of lavas from destructive plate boundaries. In *Andesites* (R. S. Thorpe, ed.). John Wiley & Sons, Chichester, 525–47.

Sang, L. and You, Z. (1988) The metamorphic petrology of the Susong Group and the origin of the Susong phosphorite deposits, Anhui Province. *Precambrian Res.*, **39**, 75–76.

—— Chen, Y., and Shao, G. (1987) Characters of quartz-keratophyres formation and their Rb–Sr isotopic ages in the southwestern part of Anhui Province (in Chinese). *Acta Petrologica Sinica*, **1**, 56–63.

Suo, S., You, Z., Zhu, B., and Liu, W. (1988) Tectonic style and deformational sequence of Dabie metamorphic terrane (in Chinese). *Earth Science—Journal of China University of Geosciences*, **13**(4), 341–9.

Tao, Q., Dong, J., Yuan, X., and Ying, J. (1986) Geochronology of Precambrian sequences in Northeastern Hubei, China (in Chinese). *Bull. Tianjin Institute, Geol. Min. Res.*, **16**, 75–89.

Wood, D. A. (1980) The application of a Th–Hf–Ta diagram to problems of tectonomagmatic classification and to establishing the nature of crustal contamination of basaltic lavas of the British Tertiary Volcanic Province. *Earth Planet Sci. Lett.*, **50**, 11–30.

Xu, S., Dong, S., Zhou, H., and Chen, G. (1986) Tectonic slides and thrusts in Dabie Mountain, Anhui Province (in Chinese). *Proc. Internat. Symp. on Precambrian Crustal Evolution*, No. 1, Tectonic. Geological Publishing House, Beijing, 262–77.

Ying, J. (1988) Proterozoic activity and isotopic studies of rocks from Dabie Mountain. *International Symposium on Geochemistry and Mineralization of Proterozoic Mobile Belts*: Abstracts. Tianjin, **125**.

You, Z. and Yang, S. (1986) The Petrography and geological significance of some typical metamorphic rocks in Jianou Group, Fujian (in Chinese). In *Tectonic History of the Ancient Continental Margins of South China* (Wang, H., Yang, W., and Liu, B., eds). China University of Geosciences Press, Wuhan, 97–112.

[*Manuscript received 16 October 1989; revised 18 July 1990*]